Angular-Momentum Effects in Subbarrier Fusion

M. L. Halbert and *3.* R. Beene
*Oak Ridge National Laboratory**
Oak Ridge, Tennessee 37831-6368, U.S.A.

Received October 12, 1993

A nalyses of our published experimental data leading to angular-momentum distribution for siibbarrier fusion of ^{64}Ni and ^{100}Mo have been re-examined, especially in the low-ℓ region. New methods were developed for reducing the experimental data to ℓ distributions. The revised of the moments of ℓ and of the cross sections for fusion are substantially unchanged from our published results.

I. Introduction

It has been known since about 1980 that fusion of heavy ions is greatly enhanced below the Coulomb barrier compared with normal barrier-penetration expectations. Reference 1 is a review that gives many examples of this phenornenon. The excitation function for fusion of ^{64}Ni + ^{100}Mo measured[2,3] in collaboration witli a group at Washington University shows the effect clearly (Fig. 1). The barrier energy is about 142 MeV; the lowest point is at about 90% of the barrier energy. The dotted curve is the prediction of a one-dimensional-barrier-penetration calculation of a type that reproduces the fusion of light projectiles very well. Several theoretical approaches have been successful in explaining the enhancement seen in much of the excitation-function data [reviewed in 4, 5], but it cannot be said that a full understanding o' the physics is in hand even after more than a decade of hard work. In fact, the reasonable success of several rather different models shows that the underlying phenomena are not well understood.

Other types of data might be helpful in distinguishing among the many different theoretical approaches. An important tind of informationnot measured in most of the experiments is the dependence on ℓ, the angular momentum of the fusing system[6,7]. We obtained such information or the cross sections, σ_ℓ, as a function of ℓ for the fusion of ^{64}Ni and ^{100}Mo [2] using the Spin Spectrometer[8]. This paper will first review the experimental method and data from Ref. 2 and then present results from a more sophisticated analysis[9] of the same data.

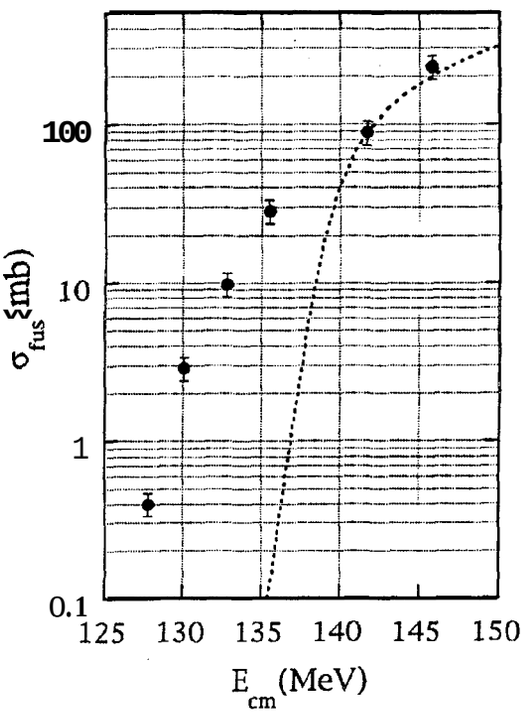

Figure 1: Experimental excitation function for fusion of ^{64}Ni + ^{100}Mo (points) compared with a calculation (curve) for penetration of a one-dimensional barrier. The highest-energy point is from Ref. 3 while the others are from Ref. 2 (as modified slightly in Ref. 9).

II. Experimental Method

The Spin Spectrometer is a segmented, closely-packed array of 72 scintillation detectors forming a nearly spherical shell, 17.8 cm thick, of NaI (Tℓ) surrounding the target[8]. Two NaI detectors were re-

*Managed by Martin Marietta Energy Systems, Inc. under contract DE-AC05-84OR21400 with the U.S. Department of Energy.

moved to allow the beam to enter and exit the shell; the beam was stopped in an externa1 Faraday cup. To identify the various exit channels, six additional NaI units were removed and replaced with Compton-suppressed Ge counters. Photopeaks due to characteristic y rays of the various residual nuclei seen in the Ge spectra were the basis for exit-channel identification and for the absolute cross sections. The photopeaks in the Ge spectra up to E_{lab} = 141.7 MeV were significant for only four channels, those corresponding to 2n, 3n, 4n, and a2n evaporations. The fusion cross sections shown in Fig. 1 were obtained by summing the yields of these four channels and a supplement of about 10% for the many other channels individually too weak to be seen in the Ge spectra. At 145.8 MeV, peaks could also be seen for the p2n, p3n, and a3n channels, and in this case measured cross sections were used for these channels[3]. The ℓ distributions (shown later) are likewise sums over the ℓ distributions for the individual exit channels. The ℓ distributions were deduced from the number of NaI detectors, k, triggered in each event in coincidence with the characteristic y-rays identified in the Ge spectrum. Again, a supplement was added for missed channels; these supplementary data were obtained from the statistical-model calculations to be described later.

We chose to study ^{64}Ni on ^{100}Mo in part because the compound nucleus, ^{164}Yb, and the residual nuclei remaining after evaporation of a few neutrons, are good rotors. The final stage of deexcitation in such nuclei is a cascade consisting of as many as 20 stretched E2 y rays. These so-called "yrast" γ rays each carry away two units of angular momentum but essentially no thermal energy. There will also be about four so-called "statistical" y rays in each cascade; they carry off thermal energy but not much angular momentum. Thus, if one measures the number of γ rays emitted (the y-ray multiplicity, m), one can deduce the spin of the residual nucleus before the y-ray cascade occurred. This spin can in turn be related to the entrance-channel angular momentum, ℓ, by adding back the angular momentnm removed by the evaporated particles. The estimates of angular momentum removal by particle evaporation and statistical y-ray emission are provided by the statistical model.

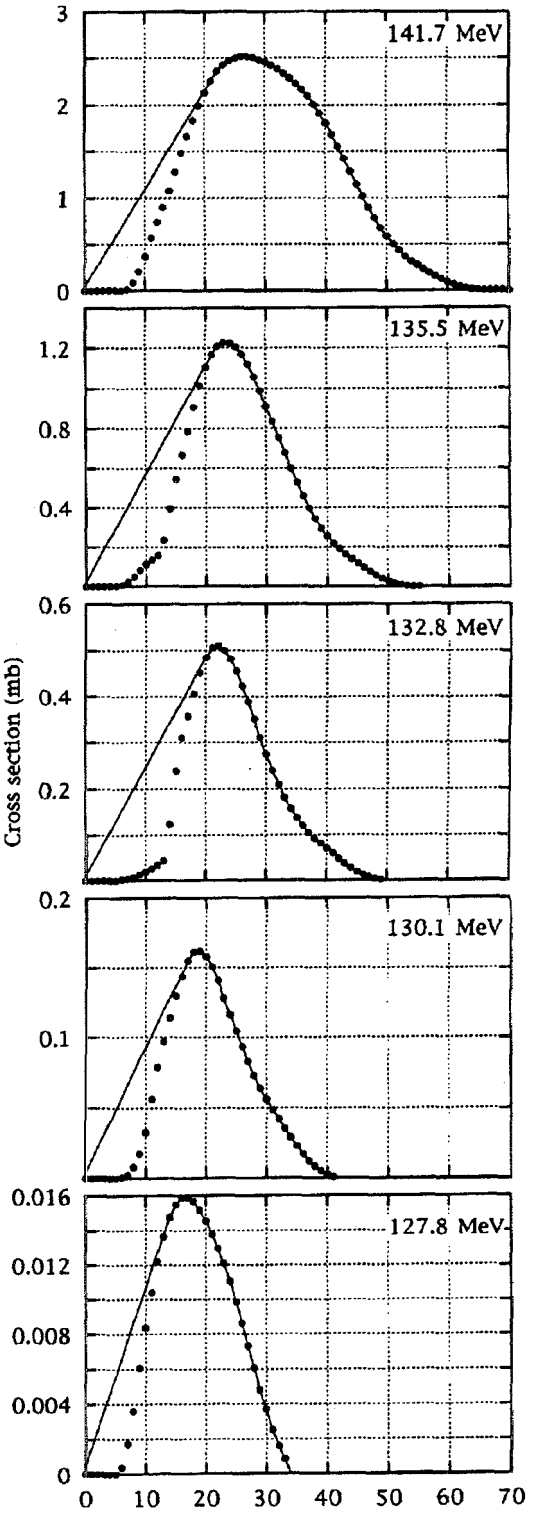

Figure 2: Experimental ℓ distributions from Ref. 2 for ^{64}Ni + ^{100}Mo (points) and a constant-T_ℓ extrapolation on the low-ℓ side.

There are some experimental complications that need to be considered. What we want is the number of y rays per event, m, but what we measure is k, the number of NaI scintillators triggered per event. A single γ ray cin be scattered from one detector to another, thereby triggering more than one detector. On the other hand, it is possible that more than one y ray may be registered in one scintillator, which is experimentally indistinguishable from detection of a single γ ray. Methotls have been developed for measuring[8] or calculating[9] the k $\rightarrow$ m response of the Spin Spectrometer. A second complication is that NaI is an efficient detector of neutrons, so we must devise some way to identify pulses due to neutrons in the Spin Spectrometer and negate their effect on the measured k distribution. In Ref. 2 the neutrons were rejected by time of flight with reference to the zero time, to, of a given event; to was determined by an iterative average of the NaI times[8]. However, events with $k < 3$ do not provide a sufficiently good estimate of to; they were discarded in Ref. 2, causing a loss of data for those evaporation channels populating mainly low angular-momentum states. The points in Fig. 2 show the E distributions we deduced in Ref. 2 from the data with the $k < 3$ rejection. To compensate for the losses at the lowest ℓ values, we assumed in Ref. 2 that the transmission coefficients, T_ℓ, below the peak of each dashed curve were ir dependent of ℓ; then we extrapolated from tlie peak reg on down to $E = 0$ (full lines in Fig. 2).

The ℓ distributions (or their first and second moments) were compared[2] with predictions from a number of theories. We found that at energies below the barrier, the theories generally predicted much smaller moments than were obtained from the extrapolated curves. Fig. 3 shows a comparison of the moments from Ref. 2 (open circles), as a function of bombarding energy, with the predictions of a coupled-channels calculation[10] taking into account the known inelastic couplings of ^{64}Ni and ^{100}Mo. (The full points in Fig. 3 are from the new analyses discussed below.) The uncertainties in the low-ℓ region and in the conversion from k to ℓ have been blamed[11] for the discrepancy with theory, but it is difficult to see how any reasonable alternative to the shape of σ_ℓ at low E could make a significant reduction in $< \ell >$, and $< E^2 >$. Nevertheless, it seemed important to us to re-examine the primary coincidence-fold data and the methods of conversion to the σ_ℓ distributions. Section III deals with re-analyses of the primary k distributions while Sec. IV outlines two improved methods of converting from k to E distributions.

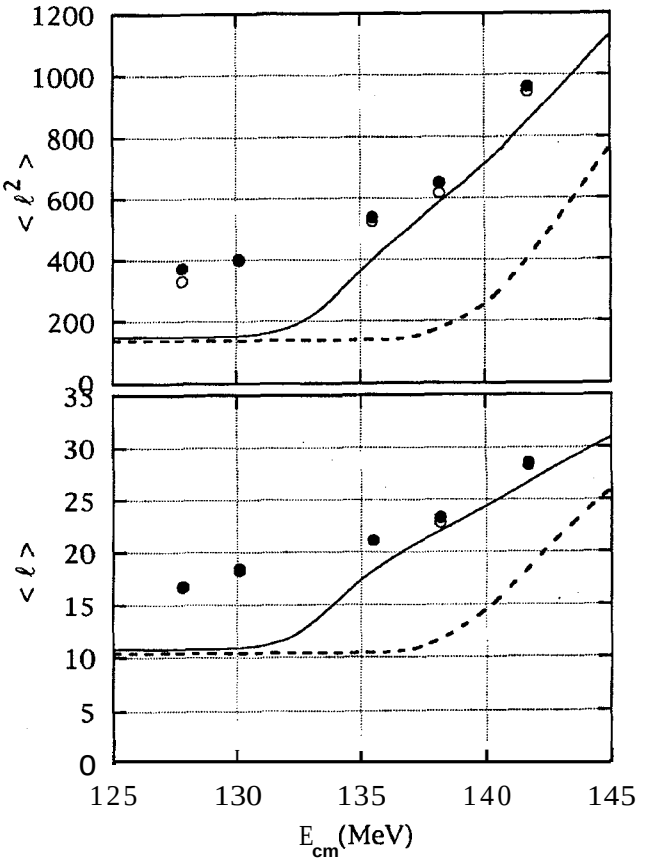

Figure 3: First and second moments of ℓ distributions. Values derived from experiment are shown by the full points, for the new analyses by the unfolding method, and by the open points, for the constant - T_ℓ extrapolations shown in Fig. 2. (For $< C >$, the two sets of results are almost indistinguishable). Theoretical predictions are shown by the curves: the dashed curve is from one-dimensional barrier penetration while the full curve is from a coupled-channels calculation[2] having inelastic couplings taken from known data on ^{64}Ni and ^{100}Mo.

III. Re-Analysis of Experimental k Distributions

We have generated new k distributions at the five ^{64}Ni beam energies of Ref. 2 by a scan of all the primary data tapes without any "filtering," i.e., without $k < 3$ rejection and without any attempt to reject NaI pulses due to neutrons. The gate on NaI times was wide enough to insure that no pulses due to prompt y rays

were excluded. Fig. 4a shows an example of the resulting "raw" or "unfiltered" k distribution (dots) for the 4n channel at $E_{lab} = 141.7$ MeV in comparison with the result of a scan of the same data tapes with neutrons and $k < 3$ events filtered out as in Ref. 2 (open circles). Figs. 4b and 4c are a similar pair of distributions for the 3n channel at 132.8 and 130.1 MeV.

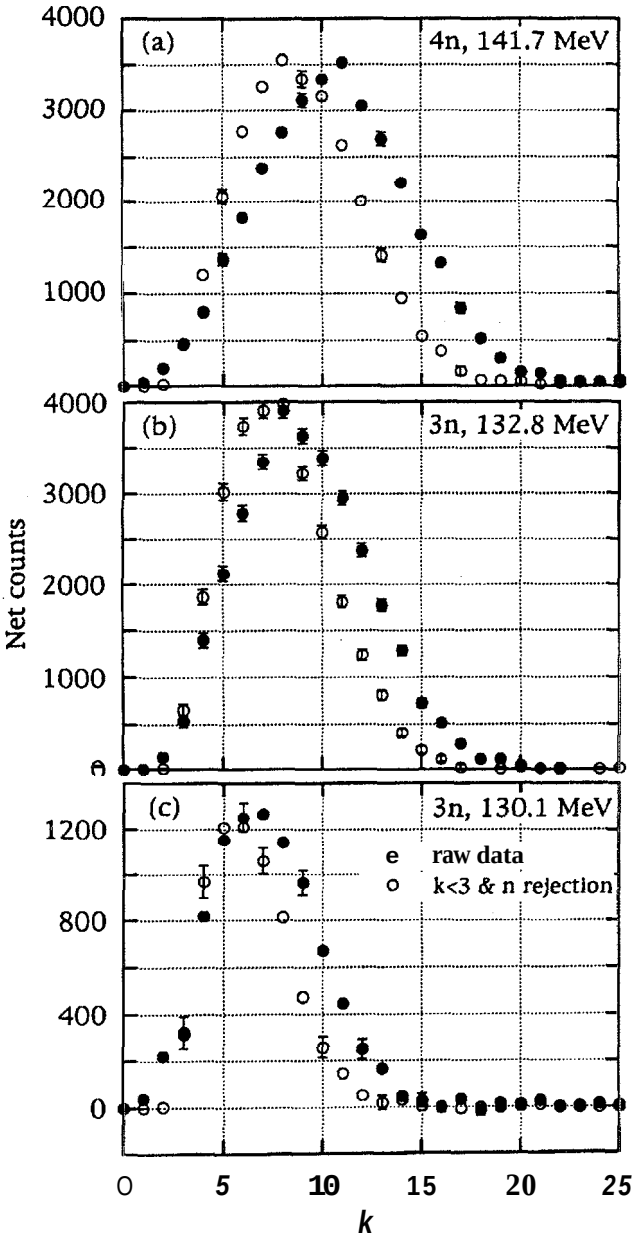

Figure 4: k distributions for the raw data (full points) and after rejection of late-arriving pulses and events with $k < 3$ (open points).

In each part of Fig. 4 the shape of the peak and the region above it are nearly the same, but the unfiltered data are moved upscale by one or two units of k due to the incliision of neutrons. In Fig. 5, the same data are replotted with the raw distribution shifted down to achieve the best match on the high side of the peak. The determination of the best-fit E shifts and the uncertainties were made by a least-squares procedure using only the data for those values of E at the peak and above. Fig. 6 shows the k shifts obtained in this way for each channel at the five ^{64}Ni bombarding energies.

The shift in k depends on the NaI neutron-detection efficiency, which is a function of the neutron energy for each exit channel and bombarding energy. Statistical-model estimates[12] of the average neutron energies were coupled with empirical determinations of the neutron efficiency of the Spin Spectrometer NaI elements[13] and the energy dependence of the neutron efficiency of 3 × 3-inch NaI cylinders[14]. The expected number of detected neutrons was found to be in reasonable qualitative agreement with the measured k shifts for various exit channels and beam energies.

A careful examination of Fig. 5 reveals that the upper side of the peak in the filtered distributions is slightly steeper than it is in the raw data. This is because the detection of neutrons by the Spin Spectrometer does not result in a fixed contribution to k. The response to neutrons, like that to y rays, is a statistical effect with a well-defined mean, but a finite width. In fact, contributions to the response function due to secondary and tertiary inelastic scatterings are more important for neutrons than for y rays since (a) evaporation neutrons have a longer mean free path in NaI, and (b) a scattered neutron is usually deflected to a larger angle than a scattered y ray. For a given exit channel, the result of adding the neutron and y-ray folds event by event is, in effect, the convolution of the y-ray fold distribution with the response of the Spin Spectrometer to the (fixed) number, x, of neutrons emitted in coincidence. This leads to a broadening of the Spin-Spectrometer response, especially on the high-k side. The determination of the best-fit k shifts allowed for the finite width of the neutron response and the consequent broadening.

Fig. 5 shows that the data to which the $k < 3$ and time-of-flight filtering was applied (open points) are deficient in counts at small k values. The unfiltered data from the new analysis (solid points) are therefore preferable at low k. On the other hand, the broadening seen at high k in the new analysis is an artifact due to

the acceptance of neutrons. It need not be tolerated because the time-of-flight neutron rejection works very well at high k. We have therefore constructed the final k distribution for each exit channel by smoothly joining the lower part of each shifted raw distribution with the upper part of the corresponding filtered distribution. The transformation and unfolding procedures described in the next sections were applied to these composite k distributions.

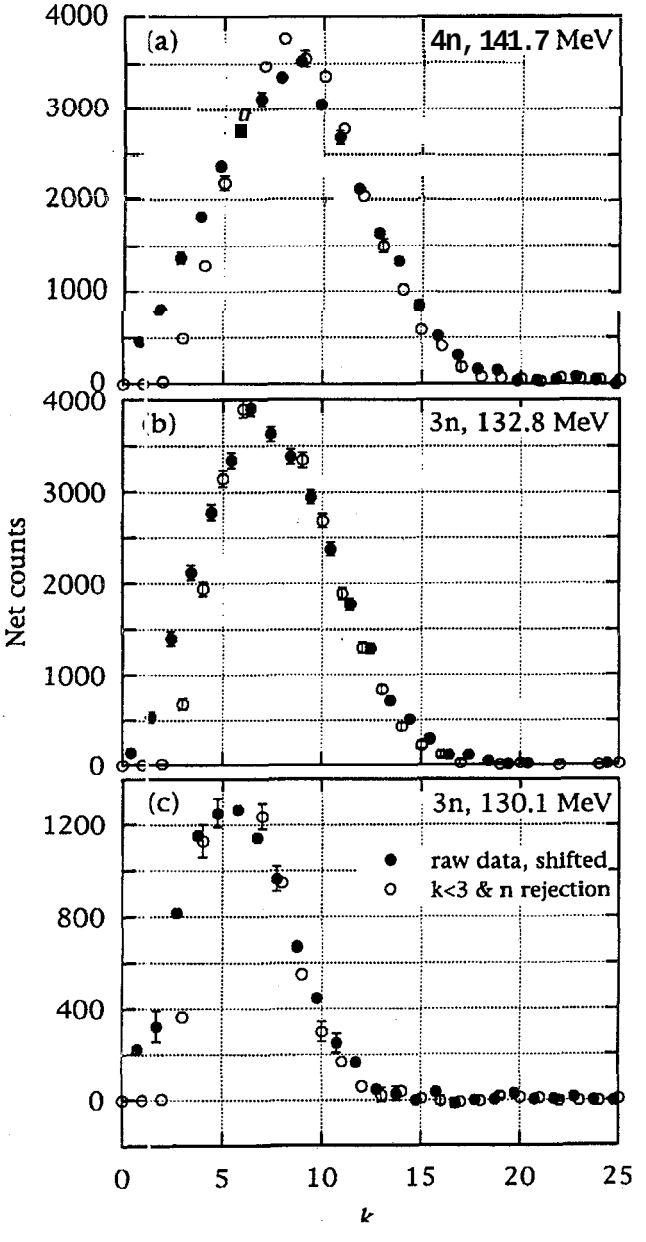

Figure 5: Same as Fig. 4 except that the raw data have been shifted down to match the upper side of each peak as a way of eliminating pulses due to neutrons.

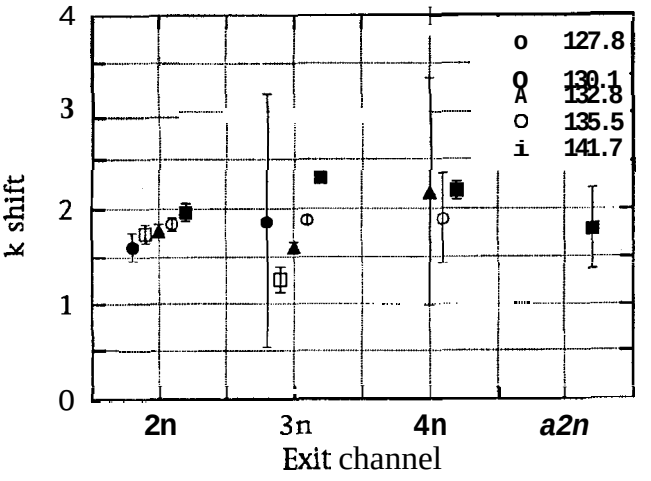

Figure 6: Fig. 6. Best-fit k shifts from data for all channels at all energies.

IV. Methods of converting k distributions to C distributions

A. General outline of methods

Our goal is to obtain the C distributions from the k distributions for each exit channel x, which we refer to as the $k_x \rightarrow C$, conversion, and then combine these, weighting each channel according to its measured cross section. Historically, this has been done in a two-step process $k, \rightarrow$ m, $\rightarrow \ell_x$ for each x. This is a reasonable partitioning of the problem, since the response of the Spin Spectrometer has been well characterized experimentally[8], and elegant methods have been applied to the $k, \rightarrow m,$ transformation[15]. In Refs. 8 and 15, the authors speak of "unfolding" the k distribution to obtain the multiplicity distribution; i.e., solving the matrix equation

$$\mathbf{K}_x = \mathbf{R}^M \mathbf{M}_x \qquad (1)$$

for the vector $M,$. In this equation, K, is a vector whose components are proportional to the yield at a given value of k, M, is the corresponding vector for the multiplicity distribution, and $\mathbf{R}^M$ is the fold-to-multiplicity response matrix which (in a somewhat more general form) has been discussed in Ref. 15. The constants of proportionality are adjusted to make the vectors sum to unity so that the components of K, and $M,$ form discrete distributions.

Generally, the $m, \rightarrow \ell_x$ transformation has been treated. much more schematically. Based on a large

body of data on fusion reactions, a simple relation between the mean angular momentum deposited in the compound system, $< \ell >$, and the mean number of rays emitted in the subsequent decay cascade, $< m >$, has been established empirically[6]:

$$< \ell > \approx a(< m > - b) , \qquad (2)$$

with a ranging from $\sim$ 1.5 to 2 and b typically in the range 3 to 5. This relation can be understood in terms of the physics of compound-nucleus decay as outlined in Sec. II. The constant a is interpreted as the average multipolarity of the stretched transitions, and b can be related to the average number of statistical y-ray transitions (i.e., those that carry away energy of excitation, but little net angular momentum). In almost all previous work, it has been assumed that a function (usually a linear relation) could be written down relating the variables ℓ and m

$$\ell = f(m) \qquad (3)$$

It is important to note that Eq. 2 is a relationship between the moments of distributions, and not the function relating variables specified in Eq. 3. This subtlety is widely ignored.

Using statistical models, more detailed relations of the type of Eq. 2 can be constructed. The initial angular momentum, ℓ, is an input parameter to the model so that equations relating ℓ and $< m >$ (still the moment of a distribution) can be constructed taking explicitly into account the angular momentum carried off by particle evaporation and other effects[2], and even the dependence of these processes on ℓ[16]. A simpler procedure is to relate the values of ℓ and $< m >$ from a statistical-model calculation by fitting them to an empirical polynomial. In this way we obtain a relationship

$$\ell = f_x(< m >) \qquad (4)$$

and make the approximation that this can be used in place of the function relating m and ℓ in Eq. 3. The subscript x is added to emphasize that we do this separately for each exit channel. We will refer to the method of using the relation f, in Eq. 4 to obtain the ℓ distribution as the "transformation method" to distinguish it from the "unfolding method" described below.

The replacement of the rather complex relationship between distributions in m and ℓ by a one-to-one mapping arrived at by relating ℓ to $< m >$, can, in principle, lead to serious distortions of the resulting ℓ distribution. It is actually unnecessary to make this approximation. Once the decision is made to base the relationship between ℓ and $< m >$ on the statistical model, one might as well use the statistical model to provide the full ℓ to m response matrix, $\mathbf{R}^L$, of the nuclear cascade. We then have the problem of solving

$$\mathbf{M}_x = \mathbf{R}^L \mathbf{L}_x , \qquad (5)$$

which is analogous to that already solved in Eq. 2. The "unfolding method" is simply the solution of this matrix equation for L_x, a vector (defined at integer ℓ values) whose components are proportional to the ℓ distribution.

There is, of course, no reason to carry out the conversion of k distributions to ℓ distributions in two steps, unless the m distributions themselves are of interest. Provided a relation equivalent to Eq. 4 relating ℓ and $< k >$ can be obtained or an overall response matrix equivalent to the product of the Spin Spectrometer and decay-cascade response, $R_x = \mathbf{R}_x^L \mathbf{R}_x^M$, can be constructed, either the transformation method or the unfolding method can be applied in a single step to produce ℓ distributions from k distributions. In the unfolding method, this is accomplished by solving for L_x in the equation

$$K_x = \mathbf{R}_x \mathbf{L}_x . \qquad (6)$$

Application of the unfolding method requires some care. The obvious approach of inverting R_x and multiplying Eq. 6 by the inverse $\mathbf{R}_x^{-1}$ is unstable. Statistical fluctuations in the response matrix can be amplified in the inverse matrix, leading to large and unphysical fluctuations in the result. We have chosen to solve Eq. 6 by the iterative improvement method[17,18], using the result of the transformation method as the first approximation to L_x. The particular iterative improvement algorithm employed was taken from Gastinel[18], and has been used for purposes similar to ours by Sørensen[15]. We should add that both R_x and K_x are subject to statistical uncertainties; the solution for L_x is therefore not unique, but the method ensures that the operation of R_x on the solution L_x produces a vector consistent

with K,. The transformation method does not provide this consistency.

B. Construction of responses

Having chosen to convert experimental data to the entrance-channel angular- momentum distribution in a single step, $k_x \rightarrow L$, we need to know how the nuclear decay cascade, together with the instrumental response of the Spin Spectrometer, converts entrance-channel angular momentum into y-ray fold. The m to k response - i.e., the Spin Spectrometer response - has been determined exper mentally[8]. We have found that this response can be reproduced extremely well with a Monte Carlo code containing an accurate representation of the Spin Spectrometer geometry. This code is based on the GEANT package[19]. Our responses were, thus, generated by a si nulation consisting of a statistical-model code (see next paragraph), which predicts the γ-ray cascade resu ting from the decay of a compound nucleus at specific L and excitation energy, and a detector response code which converted the y-ray cascade into detector hits and hence y-ray fold.

The L to m "response" has usually been obtained with the aid of statistical-model codes. This is also our approach. The statistical-model calculations were made with the code EVAP[20] which is derived from the code PACE2S[12], for the decay of ^{164}Yb at each of the excitation energies relevant to the present analysis. The missed transitions resulting from known isomers in ^{161}Yb (3n channel) and interna1 conversion in all channels were also included explicitly in the calculation. These calculations are described in Ref. 9 and will not be detailed here. The effects of varying the level-density parameter between A/7.5 and A/10 were negligible compared to statistical uncertainties. The experimental channel-selection criteria can have a significant effect on the ℓ to E response; they were therefore included in the simulation. For example, in constructing responses for the 3n channel (^{161}Yb), it was required that the yrast $17/2^+$ to $13/2^+$ y-ray transition appeared.

The funct onal relationship of the form

$$\ell = f_x(< k >) \qquad (7)$$

required for the transformation method can also be obtained from these calculations. For each channel x, the mean fold $< k >$ was calculated for each ℓ. The resulting set of pairs ℓ, $< k >$ were fit to a cubic polynomial and the transformation of k, to ℓ_x was then carried out. We emphasize again, that in order to apply the transformation method using an equation of the type of Eq. 7, we are in effect assuming that the relation between ℓ and $< k >$ can be treated as if it were a functional relationship between the variables ℓ and k. There is no justification for this assumption. The consequences of applyiing the transformation method to obtain the ℓ_x distributions - and hence assuming a one-to-one relationship between k and ℓ, when in fact the true relationship is one of broad distributions - are discussed in Sec. VB.

We should mention for completeness that the transformation method of Ref. 16 was equivalent to the present one although it differed in detail. The k to m response in Ref. 16 was the same as in Ref. 8, which is well reproduced[9] by the GEANT simulation. The m to ℓ transformation of Ref. 16 was based on statistical-model estimates of the angular momentum removed by evaporated neutrons and statistical y rays as a function of ℓ foir each exit channel; the present transformation used similar information (with better statistical accuracy). The results of the present transformations and those of Ref. 16 are practically indistinguishable.

C. Determination of σ_ℓ

Given the response matrix R, or the relationship $\ell = f_x(k)$, estimates of the ℓ distributions normalized to unity, P_x^L, were obtained for each channel separately, using (1) the unfolding method or (2) the transformation method. The partial-wave distributions for each excitation energy, σ_ℓ, were then formed by summing over the observed channel

$$\sigma_\ell = \left[\sum_x \sigma_x P_x^L(\ell)\right] C(\ell)G(\ell) \; . \qquad (8)$$

where the σ_x is the updated experimental cross section for exit channel x from Ref. 9. The factor $C(\ell)$ accounts for the fact that the statistical model predicts a nurnber of weak channels which were not included in the experimental analysis [(pn), (p2n), (αn), etc.]. For each excitation energy the numerical values of $C(\ell)$ at each value of! is the ratio of the total number of cascades initiated for that value of! divided by the number which

Ied to one of the observed channels. This method of correcting for unobserved channels is adequate so long as $C(\ell)$ is not much larger than unity.

While $C(\ell)$ corrects for unobserved channels, $G(\ell)$ corrects for missing yield in observed channels due to the experimental method used for channel identification. Ideally, channels would be identified by determining the number of residual nuclei produced in their ground states. In our experiment, the channel identification is based on characteristic y-ray transitions between states in the nucleus. Cascades which bypass the initial state of the identifying transition will be missed. If these missed cascades do not result equally from all ℓ values, there will be a bias in the shape of the σ_ℓ. $G(\ell)$ is calculated from the statistical-model data by taking, as a function of ℓ, the ratio of the total number of events populating channel x to the number of those populating channel x which also involved emission of the gating transition. This correction was significant only for the 3n channel (though it should be noted that it is applied after the individual channels are combined). Fig. 7 shows examples of ℓ distributions before (dotted lines) and after (full lines) correction for the $C(\ell)$ $G(\ell)$ factor of Eq. 8. The combined effect of these two corrections on the extracted cross sections range from 9% to 12% for the five ^{64}Ni + ^{100}Mo energies investigated here.

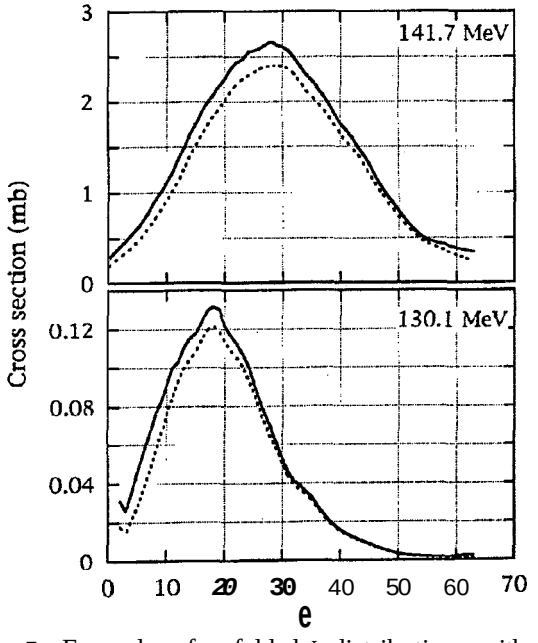

Figure 7: Examples of unfolded L distributions with (full lines) and without (dotted lines) both the corrections of Eq. 8: $C(\ell)$ for weak channels not seen experimentally and $G(\ell)$ for yield missed because the decay cascade bypasses the triggering transition.

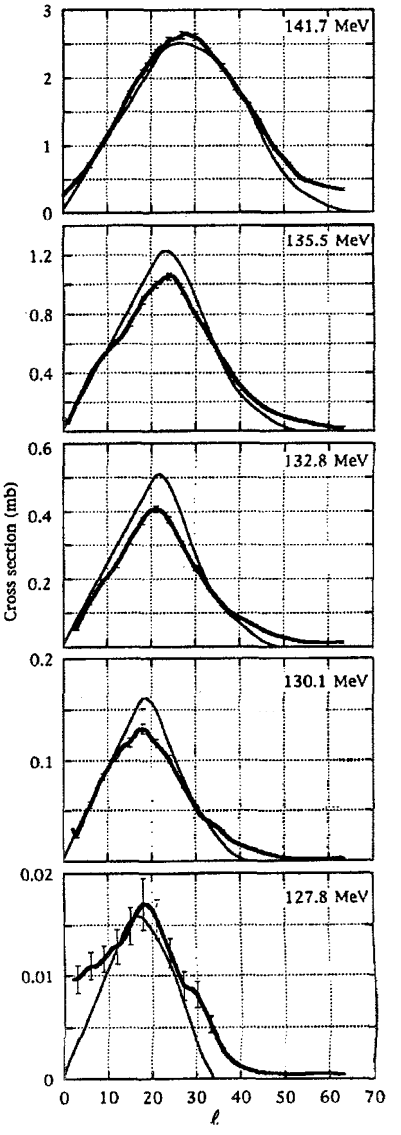

Figure 8: L distributions from the unfolding method (heavy lines) compared with the extrapolated L distributions of Fig. 2 (light lines).

V. Results for ℓ distributions

The two methods of converting k to ℓ give nearly the same results for ^{64}Ni + ^{100}Mo, despite our warning of inaccuracy in principle for the transformation method; these results are given in Secs. A and B below. In the case of ^{16}O + ^{148}Sm, the two methods actually do give different results (not shown here). This occurs because the ℓ distributions are narrower and vary significantly over a range of ℓ values comparable to the width of the response function, unlike the ^{64}Ni + ^{100}Mo case.

A. ℓ distributions from the transformation method

Table I - Moments of $< \ell >$ distributions for $^{64}Ni + ^{100}Mo$, as deduced from the primary experimental data in various approximations.

	Transformation method				Unfolding method	
$E_{c.m.}$	From Ref. 2		L dependence included			
(MeV)	$< \ell >^a$	$< \ell^2 >^b$	$< \ell >$	$< \ell^2 >$	$< \ell >$	$< \ell^2 >$
141.7	28.3	947	29.0 ± 0.4	1018 ± 16	28.5 ± 0.3	963 ± 16
135.5	22.9	617	24.1 ± 0.5	712 ± 17	23.3 ± 0.4	652 ± 17
132.8	21.1	526	22.4 ± 0.5	628 ± 18	21.1 ±0.4	539 ± 18
130.1	18.4	401	19.0 ± 0.7	459 ± 24	18.3 ± 0.5	399 ± 24
127.8	16.8	330	17.4 ± 0.8	403 ± 19	16.7 ± 0.7	373 ± 19

[a] - Uncertaiiity $\leq 5\%$.
[b] - Uncertainty $\leq 10\%$.

The composite k distributions described at the end of Sec. III were converted to L distributions for each exit channel x by means of the $k \rightarrow L$ response represented by a cubic, as explained in Sec. IVB. The L distributions for each beain energy were then summed with weights based on the experimental channel cross sections given in Ref. 9.

The first and second moments of L for these distributions are listed in columns 4 and 5 of Table I. For comparison, columns 2 and 3 repeat the original values published in Ref. 2. There is a small increase in $< L >$ and $< \ell^2 >$, for the present distributions, as already noted in Ref. 16 for a nearly equivalent transformation method.

B. ℓ distributions from the unfolding method

The heavy curves in Fig. 8 show the weighted sum of the individual distributions obtained by unfolding the k distribution for each exit channel. The five parts of Fig. 8 correspond to the five bombarding energies of Ref. 2. The weighting was based on the experimental values of the channel cross sections[9]. These curves are the final a distributions including both of the correction factors, $C(\ell)$ and $G(\ell)$, of Eq. 8. For comparison, the extrapolated ℓ distributions[2] are shown by the light curves. The new unfolding results (heavy curves) are broader and extend to higher ℓ values.

Columns 6 and 7 of Table I compare the first and second moments of ℓ for the unfolding method with those from the transformation method (cols. 4 and 5). The unfolding results are also plotted in Fig. 3 (full points). These results are based on the same response functions; the small differences between them are a measure of the accuracy of the approximation inherent in the transformation method for the $^{64}Ni + ^{100}Mo$ systems. It is interesting that the values of $< \ell >$ from the unfolding method are very close to those from the transformation method used in Ref. 2, based on the intuitive constant-T_ℓ extrapolations at the low L values. This can also be seen in Fig. 3, where the results of the extrapolations can hardly be distinguished from the new results, at least for the first moment. The second moments of the new analyses are larger than those of Ref. 2 since the ℓ distributions extend to higher L valiies (as is clear from Fig. 8).

VI. Comparisons of $< L >$ with theory

In Ref. 2, the only theoretical calculations that came close to the experimental $< \ell >$ well below the barrier were those which depend significantly on empirical adjustments. For example, the radius of the imaginary potential for fusion in Ref. 21 is meant to be varied to fit the data. In our case a reasonable fit was obtained[2] with the rather large radius parameter $r_0 = 1.44$ fm, which corresponds to fusion occurring at unconventionally large distances (under the barrier or even outside of it).

A number of reasonably successful attempts to fit our results for $< L >$ have been submitted for publication very recently. Among these are a calculation of one- dirnensional barrier penetration[22] for an energy-dependent barrier[23], a coupled- channels calculation in the rotating frame approximation[24], and a multi-dimensional model of the fusion process that takes into account the deformations of the ions during subbarrier tunneling[25]. It should be mentioned that in the first

case, the input to generate the energy-dependent barrier was taken from the experimental C distributions of Ref. 2, so the success in reproducing the C distributions is probably to be expected. Coupled-channels calculations are also presented in Ref. 22; by adding additional couplings in an empirical fashion, the moments of ℓ can be reproduced better than in Fig. 3 although the lowest-energy point is still underpredicted. In Ref. 24, inclusion of two- phonon excitations in addition to one-phonon excitations improves the agreement with experiment substantially.

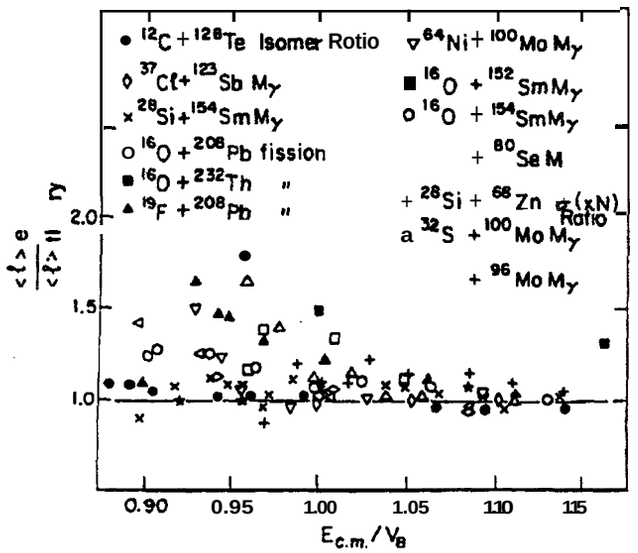

Figure 9: Ratio of experimental $< \ell >$ to the coupled-channels result for a variety of experiments, plotted as a function of c.m. bombarding energy divided by the barrier energy.

Vandenbosch[6] presented a summary plot of all the experimental information available through 1991 on angular momentum distributions; this is reproduced here as Fig. 9. Four different experimental methods were used to determine $< C >$. The ordinate is the ratio of the measured $< \ell >$ to that predicted by a coupled-channels calculation. The abscissa is the c.m. energy divided by an estimate of the barrier. The agreement of the coupled-channels theory with experiment is generally satisfactory above the barrier, but below the barrier the theory tends to underpredict $< \ell >$ for the reactions with the largest values of $Z_1 Z_2$. Vandenbosch points out that such systems have the largest density overlap at the internuclear separation corresponding to the top of the barrier. They might thus be more subject to redistribution of mass during the collision, with consequent changes in the reduced mass of the entrance channel which are not explicitly considered in the coupled-channels calculations. Mass redistribution during fusion leading to neck formation has been considered in several theoretical papers[26–30]. The calculations are very difficult; even if the projectile and target are identical, simplified parameterizations of the di-nuclear shape are required for the calculations to be tractable. Enhancements of σ_{fus} are predicted by all the calculations. In the two papers that show ℓ distributions[27,29], it is clear that large ℓ values are more important than in the case of one-dimensional barrier penetration. It is encouraging that such calculations seem to be going in the right direction for better agreement with experiment.

References

1. M. Beckerman, Phys. Rep. 129, 145 (1985).
2. M. L. Halbert, J. R. Beene, D. C. Hensley, K. Honkanen, T. M. Semkow, V. Abenante, D. G. Sarantites and Z. Li, Phys. Rev. C40, 2558 (1989).
3. J. L. Barreto, N. G. Nicolis, D. G. Sarantites, R. J. Charity, L. G. Sobotka, D. W. Stracener, D. C. Hensley, J. R. Beene, M. L. Halbert and C. Baktash, Phys. Rev. C (in press).
4. S. G. Steadman and M. J. Rhoades-Brown, Ann. Rev. Nucl. Part. Sci. **36,** 649 (1986).
5. M. Beckerrnan, Rep. Prog. Phys. 51, 1047 (1988).
6. R. Vandenbosch, Ann. Rev. Nucl. Part. Sci. 42, 447 (1992).
7. R. R. Betts, Proc. Int. Symp. Towards a Unified Picture of Nuclear Dynamics, Nikko, Japan, 1991 (Amer. Inst. Phys. Conf. Proc. 250, New York, 1991).
8. M. Jääskeläinen D. G. Sarantites, R. Woodward, F. A. Dilmanian, J. T. Hood, R. Jääskeläinen, D. C. Hensley, M. L. Halbert and J. H. Barker, Nucl. Ins. Meth. 204, 385 (1983).
9. M. L. Halbert and J. R. Beene (to be published).
10. C. H. Dasso and S. Landowne, Comput. Phys. Comm. 46, 187 (1987).
11. C. H. Dasso, in Nuclear Structure and Heavy-Ion Reaction Dynamics 1990, edited by R. R. Betts

and J. J. Kolata, Institute of Physics Conference Series Number 109 (1991), pp. 293-4.

12. A. Gavron, computer code PACE2, Phys. Rev. C**21**, 230 (1980); and private communication; J. R. Beene, modification PACE2S.
13. Z. Majka, N. Abenante, Z. Li, N. G. Nicolis, D. G. Sarantites, T. M. Semkow, L. G. Sobotka, D. W. Stracener, J. R. Beene, D. C. Hensley and H. C. Griffin, Phys. Rev. C 40, 2124 (1989).
14. O. Hausser, M. A. Lone, T. K. Alexander, S. A. Kushneriuk and J. Gascon, Nucl. Instr. Meth. Phys. Res. **213**, 301 (1983).
15. S. P. Sørensen, Nucl. Phys. A**461**, 487c (1987).
16. M. L. Halbert and J. R. Beene, in Proceedings of the KIV Symposium on Nuclear Physics, Cuernavaca, Mexico, January 7-10, 1991, edited by M.-E. Brandan (World Scientific, Singapore, 1991), p. 105.
17. W. H. Press, B. P. Flannery, S. A. Teukolsky and W. T. Vetterling, Numerical Recipes (Cambridge University Press, Cambridge, 1986), Chapter 2.7.
18. N. Gastinel, Linear Numerical Analysis (Academic, New York, 1970). See 5.16 and 5.21.
19. R. Brun, F. Bruyant, M. Maire, A. C. McPherson and P. Zanarini, GEANT 3 User's Guide, PD/EE/84-1, CERN (1987).
20. N. G. Nicolis, D. G. Sarantites and J. R. Beene (unpublished).
21. T. Udagawa, B. T. Kim and T. Tamura, Phys. Rev. C 32, 124 (1985); B. T. Kim, T. Udagawa and T. Tamura, Phys. Rev. C**33**, 370 (1986).
22. N. Nicolis and D. G. Sarantites (submitted for publication).
23. A. K. Mohanty, S.V.S. Sastry and S. K. Kataria, Phys. Rev. Lett. 65, 1096 (1990).
24. K. E. Rehm, H. Esbensen, J. Gehring, B. Glagola, D. Henderson, W. Kutschera, M. Paul, F. Soramel and A. H. Wuosmaa, Phys. Lett. B (in press).
25. V. Yu. Denisov and G. Royer (submitted for publication).
26. li. J. Krappe, K. Mohring, M. C. Nemes and H. Rossner, Z. Phys. A**314**, 23 (1983).
27. A. Iwamoto and K. Harada, Z. Phys. A**326**, 201 (1987).
28. J. Schneider and H. H. Wolter, Z. Phys. A**339**, 177 (1991).
29. C. E. Aguiar, V. C. Barbosa, L. F. Canto and R. Donangelo, Nucl. Phys. A**472**, 571 (1987).
30. V. S. Ramamurthy, A. K. Mohanty, S. K. Kataria and G. Rangarajan, Phys. Rev. C**41**, 2702 (1990).